Wavelet-based Narrowband Interference Suppression in Long Term Evolution Physical Channels

João Paulo Miranda, Dick Melgarejo, Fabiano Mathilde, Felipe A. P. de Figueiredo, and Juliano João Bazzo
Centre for Research and Development in Telecommunications (CPqD), Campinas/SP, Brazil
Email: [jmiranda, dickm, fabianom, felipep, jbazzo]@cpqd.com.br

***Abstract*—The interference caused by a narrowband system on another system that transmits wideband or spectrally spread signals is, in general, a known problem in wireless communications. However, analyses found in the literature often model the signal of interest as a *generic* transport channel whose subcarriers convey information of the same kind. This does not reflect the specific structure and nature application of signals conveyed through the different *physical* channels of the Long Term Evolution (LTE) standard. Having the candidacy of wavelets as adequate means to mitigate narrowband interference (NBI) in *both* the user *and* control planes of LTE previously confirmed in [9], in this paper we extend our analysis to different wavelet types and operation conditions. Biorthogonal, Coiflets, Daubechies, and Haar wavelets are put to the test with respect to their ability to suppress NBI in the LTE downlink. Our simulations suggest that an optimised wavelet-based NBI suppression process calls for different wavelet types, the choice of which being dependent of the LTE physical channel considered. Daubechies are shown most convenient for synchronization channels, while Coiflets are found to be the best option when it comes to data shared channels.**

I. Introduction

Narrowband interference (NBI) is the interference caused by a narrowband wireless communication system on another wireless communication system that uses wideband or spectrally spread signals. The effects of NBI manifest themselves as a wideband receiver within the coverage area of a narrowband transmitter does *not* pick up the noisy signals of interest (SOI), *but* a sum of SOI, narrowband signals and noise instead. Depending on the transmit power of the narrowband system, the undesired components present in the sum signal may introduce nonlinear distortions in the automatic gain control and analog-to-digital conversion blocks of the wideband receiver. This is a well understood issue, and ways to tackle it are known for NBI of both non-intentional nature [1]–[6], and intentional nature, $e.g.$ jamming in military communications [7][8].

Narrowband systems may be found operating in frequencies designated for Long Term Evolution (LTE) systems, especially in bands where legacy (non-LTE) systems are in the process of being refarmed. Up until the point where spectrum refarming is complete, however, there is a need for LTE and narrowband systems to coexist. This need is better understood with the aid of an example. Consider the Band 31, a LTE band recently standardized by Third Generation Partnership Project (3GPP). Our field measurements reported in [9] confirmed the presence of multiple narrowband systems in both uplink (452.5–457.5 MHz) and downlink (462.5–467.5 MHz) LTE frequencies. Figure 1 shows a smaller set of findings for the downlink.

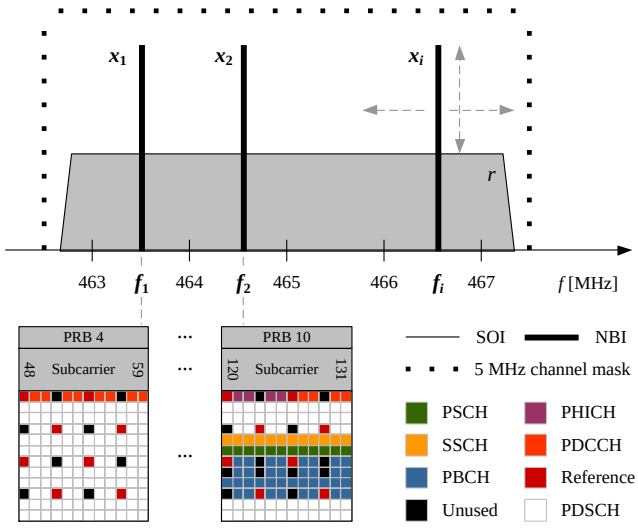

Fig. 1. Exemplary scenario of NBI in the LTE downlink. The signals x_1 and x_2 are real-world narrowband signals found in the Band 31. The signal x_i is an artificially-created narrowband signal that introduces controlled NBI.

The narrowband signals x_1 ($@f_1 = 463.5500$ MHz) and x_2 ($@f_2 = 464.6000$ MHz) overlap different portions of the received LTE signal r. x_1 mainly affects data on the user plane, $i.e.$ the physical downlink shared channels (PDSCH), whereas x_2 mainly affects control plane information. In particular, x_2 has potential to disrupt the Zadoff-Chu sequences conveying symbol timing and frequency offsets in the primary synchronization channels (PSCH). If so the LTE receiver fails to get time synchronized with the system, thus making it hard to extract frame timing and cell identity information transmitted in the secondary synchronization channels (SSCH). Lack of the aforementioned information prevents the correct access on the part of the LTE receiver to basic operation parameters, $e.g.$ channel bandwidth, cyclic prefix (CP) length, and antenna mode, transmitted in the physical broadcast channels (PBCH). As a consequence, the cell search procedure gets compromised and the receiver cannot register with the cell [10].

It becomes evident from the above example that the analysis of NBI (and approaches to alleviate its deteriorating effects in the system performance) calls for modeling that takes *physical* channels into consideration. However, the literature on NBI has not managed so far to address this aspect, as most analyses typically rely on the assumption of a *generic* transport channel where all SOI subcarriers convey information of the same kind

[1]–[8]. In answer to this need, we present in [9] a standard-compliant assessment of the NBI suppression performance of some promising time-frequency distributions (TFDs). Among the TFDs evaluated therein, Daubechies wavelets are shown to offer the best compromise in terms of complexity and signal distortion regardless the type of physical channel.

Having confirmed the candidacy of wavelets as an adequate tool to mitigate NBI in LTE physical channels in our previous work, in this paper we extend the analysis to different wavelet types and operation conditions. Here, Biorthogonal, Coiflets, and Haar wavelets are evaluated in addition to Daubechies with respect to their ability to suppress NBI in the LTE downlink. It turns out from our simulation work that an optimised suppression process calls for different wavelet types, the choice of which being dependent of the physical channel considered. Daubechies are shown most convenient for synchronization channels (PSCH and SSCH), while Coiflets are found to be the best option when it comes to data shared channels (PDSCH).

The remainder of the paper is organized as follows. Section II introduces the system model, overviews the fundamentals of NBI suppression, and details the process for the specific case of wavelets. Simulation results are then presented in Section III, where the major contributions of the paper are discussed. Conclusions are offered in Section IV.

II. System Model

Let N_{S} denote the number of subcarriers, $C_f(e)$ the complex constellation transmitted by the eth subcarrier during the fth symbol, Δf the subcarrier spacing, T_{CP} the length of the cyclic prefix, T_{S} the sampling period. The LTE downlink Orthogonal Frequency-Division Multiplexing (OFDM) signal conveyed by the fth symbol is given by

$$s(t) = \sum_{e=-\lfloor N_{\mathrm{S}}/2 \rfloor}^{\lceil N_{\mathrm{S}}/2 \rceil} C_f(e) \exp\left(j2\pi\Delta f e(t - T_{\mathrm{CP}}T_{\mathrm{S}})\right), \quad (1)$$

with a physical resource block (PRB) formed by grouping F consecutive symbols into a block of E consecutive subcarriers, and $C_f(0) = 0$. Resource grid, physical signals and channels are then generated in detailed accordance to the standard [11]. In what follows, by abuse of notation, we shall refer to (1) as the SOI associated with a generic but standard-compliant LTE physical channel.

Suppose the SOI now becomes corrupted by $i = 0, \ldots, I$ narrowband signals. NBI sources statistically relevant in terms of transmit power and talk time were shown in [9] to be push-to-talk (PTT) radios for the case of the Band 31. The signals transmitted within such systems can be assumed, without loss of generality, based on frequency modulation (FM). Under this assumption, the FM signal transmitted by the ith NBI source can be written as

$$x_i(t) = A_i \cos\left[2\pi f_i t + 2\pi f_{\mathrm{dev}} \int_0^t a_i(u)du + \theta_i\right], \quad (2)$$

where A_i, f_i, and f_{dev} are the magnitude, center frequency, and frequency deviation of the carrier used to modulate the audio signal $a_i(t)$, and the random phase θ_i is uniformly distributed in the interval $(0, 2\pi)$.

After being passed through a multipath fading channel with impulse response $h[l]$ and L taps, the signal picked up by the LTE receiver (assumed not desensitized) corresponds to

$$z[n] = r[n] + \sum_{i=0}^{I} y_i[n] + w[n], \quad (3)$$

where $r[n]$ and $y_i[n]$ are filtered versions of (1) and (2), $i.e.$ $r[n] = \sum_{l=0}^{L-1} h[l]s[n - \sigma_l]$ and $y_i[n] = \sum_{l=0}^{L-1} h'[l]x_i[n - \sigma_l]$, σ_l is the channel delay spread associated with the lth channel tap, and $w[n]$ is additive white Gaussian noise (AWGN) statistically independent from tap to tap. Note that, in contrast to the static (and probably band specific) NBI scenario discussed earlier, the narrowband signals in (2) and (3) can be modified in terms of number, magnitude, and position. This allows the different LTE downlink physical channels to be fully exercised in the absence or presence of controlled NBI, $e.g.$ as illustrated by the narrowband signal x_i in Figure 1.

A. Fundamentals of NBI Suppression

Most NBI suppression techniques have as their basis some sort of three-step process. The first step is the decomposition of $z[n]$ into some transform domain where the signal components corresponding to the NBI can be more easily identified. In case SOI and narrowband signals are distinguishable in the selected domain, the components due to the latter can be estimated via maximum likelihood (ML) [1], linear minimum mean square error (MMSE) [2], or a combination of compressive sensing and weighted least squares [3]. The second and third steps respectively involve the removal of such undesired components, and the reconstruction of an estimate of $z[n]$, $\hat{z}[n]$.

A generic representation of this process can be found in Figure 2. The analysis block outputs the channel set $Z_k[m]$, $k = 0, 1, \ldots, K-1$, which is fed into the suppression block. After the narrowband signals $y_i[n]$ have been estimated and cancelled out, $\hat{Z}_k[m]$, $k = 0, 1, \ldots, K-1$, channels are made available for the synthesis block. This block reconstructs the noisy SOI, thus bringing the solution back to the original problem domain. To keep signal distortion low, the reconstructed signal $\hat{z}[n]$ should provide a good approximation of (3) when $I = 0$, $i.e.$ as in the no NBI case.

Excision approaches exploit the fact that NBI often comes into play as high-power signals that can be distinguished from lower-power SOI in the frequency domain. Robustness against narrowband signals with center frequencies that change over time, and frequency selective fading are among their advantages. However, when the NBI spectra do not sit at frequencies coinciding with the bins of the discrete-time Fourier transform (DFT), carried out at the demodulator, spectral leakage occurs. The higher the NBI power, the larger the number of corrupted subcarriers in $\hat{z}[n]$. This issue can be circumvented by mapping the data only to those subcarriers whose powers exceed a given signal-to-interference ratio [4], but the resulting system may fail to comply with currently DFT-based wireless standards.

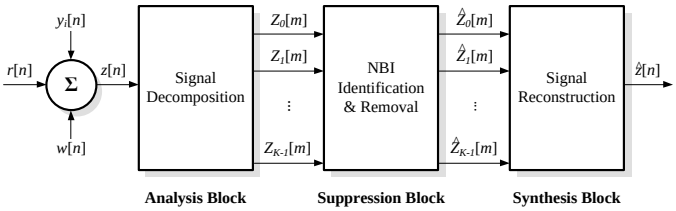

Fig. 2. Block diagram of a generic NBI suppression process.

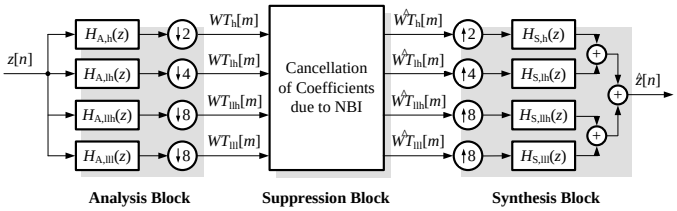

Fig. 3. Exemplary multilevel wavelet-based NBI suppression process ($J = 3$).

Techniques that operate in the time domain avoid spectral leakage by applying cancellation filters before the DFT block. Time-domain cancellers require less prior knowledge to work than their frequency-domain counterparts, $e.g.$ only estimates of the frequencies where the NBI spectrum sits at and/or its power per subcarrier. As for the limitations, performance may deteriorate in the presence of frequency offsets. This is exactly the case with phase-locked loops [5], which may undergo a further drop in performance if quadrature phase shift keying (QPSK) is in use. Care must also be taken when it comes to filter design, as impulse responses longer than T_{CP} introduce intersymbol interference (ISI).

In general, NBI suppression in frequency *and* time domains offer flexibility and resolution superior to those obtained in a single domain. Wavelet transforms [6], multirate digital filter banks (MDFBs) [7], and bilinear signal distributions [8], are TFDs that offer relatively lower complexity and near-perfect signal reconstruction at the expense of none or very few prior knowledge of the systems and signals causing NBI. Another advantage is that, by direct representing the frequency content of the signal while keeping the time description parameter, the linear progression of the frequency with time can be observed [12]. However, despite its potential for robustness against NBI, the application of TFDs has been limited to spectrally spread systems [6]–[8] and a better understanding is needed in the context of multicarrier wideband systems.

B. Wavelet-based NBI Suppression

In answer to the aforementioned need, we assessed in [9] the NBI suppression performance of Daubechies wavelets, a polyphase implementation of MDFBs, and a custom Wigner-Ville distribution aided time-domain canceller. Among the TFDs considered, Daubechies are shown the best compromise in terms of complexity and signal distortion regardless the physical channel type. A question that remains open is whether wavelet types other than Daubechies can improve performance further, and, if so, what type best suits each physical channel. This may well be the case since the wavelet choice is dictated by the signal characteristics (recall the distinct structure of signals conveyed through different LTE physical channels) and application nature. But before we carry on with the selection of candidate wavelets, let us briefly review their theory and an efficient way to implement a wavelet-based NBI suppressor.

The idea of the wavelet transform is to project a signal on a family of zero-mean functions $\Psi_{u,v}(t)$, $u, v \in \mathbb{Z}$, deduced from an elementary function $\Psi(t)$ by translations and dilations, $i.e.$ $\Psi_{u,v}(t) = \Psi(a_0^v t - ut_0)$. The fully representation of the received signal z using coefficients of the form [12]

$$WT_z[u, v; \Psi] = a_0^{v/2} \int_{-\infty}^{+\infty} z(t)\Psi_{u,v}^* dt \tag{4}$$

requires the number of scalling steps, a_0, and time dilations, t_0, to be infinite. Fortunately, this limitation can be overcome by exploiting the close relationship of MDFBs with the discrete wavelet transform (DWT). Using the DWT, the implementation of the analysis (synthesis) block in Figure 2 requires only a pair of lowpass and highpass filters, whose outputs are both downsampled (upsampled) by 2. In each scale obtained at the output of the bank of filters, NBI is suppressed by cancelling out the coefficients associated with narrowband components. The threshold applied to this end can be set using [6]

$$\gamma = \sigma_s^2 \sqrt{2}\, \text{erf}^{-1}(P_{\text{fa}}), \tag{5}$$

where σ_s^2 is the variance of the SOI and P_{fa} is the probability of a sample crossing γ in the absence of interference.

The multilevel DWT involves the repetitive application of uniform filter banks on the low-frequency channel, meaning that redundancy is introduced more in that channel as compared to the high-frequency channel. In such multilevel settings, finer resolution is achieved but the recursive coefficient computation raises the need to store intermediate coefficients. This burden can be avoided by replacing the cascaded lowpass filters and subsampling by 2 at each resolution level of the analysis block by an equivalent analysis filter, defined in the z-domain as [13]:

$$H_{\text{A}}^J(z) = \prod_{j=0}^{J-1} H_{\text{A}}(z^{2^j}). \tag{6}$$

An equivalent synthesis filter $H_{\text{S}}^J(z)$ can be generated accordingly to replace the cascaded highpass filters and upsampling by 2 used in the synthesis block. In either case, the coefficients of the jth level can now be computed without prior knowledge of the coefficients of the $(j-1)$th level. Such an equivalent filter implementation of the multilevel DWT is given in Figure 3 for the case of a three-level MDFB ($J = 3$).

In such an implementation, the wavelet type used at each level needs to be compactly supported, $i.e.$ to allow discrete-time analysis based on the DWT. Another requirement, determined by the application nature, is that the wavelet considered should possess the perfect reconstruction property. This led us to the candidates listed in Table I, alongside with some distinguishing characteristics [14]. Coiflets, Daubechies, and Haar

TABLE I
SELECTED CANDIDATE WAVELETS AND THEIR CHARACTERISTICS.

Wavelet Type	**Short Name**	L_{sup}	W
Biorthogonal	Bior$N_{\text{d}}.N_{\text{r}}$	$2N+1$	$\max(2N_{\text{d}}, 2N_{\text{r}})+2$
Coiflets	Coif-N	$6N-1$	$6N$
Daubechies	Daub-N	$2N-1$	$2N$
Haar	Haar	1	2

are orthogonal wavelets, for which support length (L_{sup}) and filter length (W) are determined by the number of vanishing moments (N). Biorthogonal wavelets differ from others in the table in that a different N can be used for decomposition (N_{d}) and reconstruction (N_{r}). All types considered are symmetric, except for Coiflets and Daubechies which are only approximately symmetric and asymmetric, respectively.

III. SIMULATION WORK

In this section, we discuss results obtained using a custom-built Matlab simulator that implements the LTE physical layer in detailed accordance to the standard [10][11]. The settings common to all simulation campaigns (unless mentioned otherwise) and those that are wavelet-specific are summarized in Table II. We consider the cases 'NBI Off' ($I=0$), 'NBI On' ($I=1$ without suppression), and 'WaveletType' ($I=1$ with suppression based on the corresponding type of wavelet. The latter two cases introduce NBI at f_1 = 463.5500 MHz and f_2 = 464.6000 MHz, one frequency at a time, so we can evaluate the impact on the performance of PDSCH and PSCH/SSCH. The NBI/SOI power ratio is 15 dB, corresponding to the worst-case condition observed in our measurements [9]. The narrowband signals are FM modulated. The SOI is QPSK modulated with code rate 1/3, single-antenna mode, and MMSE equalization. The number of vanishing moments used within each wavelet type is carefully chosen by means of small-scale simulations so as to produce the best results for fixed resolution ($J=8$) and probability of false alarm ($P_{\text{fa}}=0.01$). 5×10^7 Monte Carlo trials are carried out for each SNR point.

A. AWGN Channel

In our first simulation campaign, we assess the performance of wavelet-based NBI suppression in the presence of AWGN. Such an evaluation scenario, where additive noise and NBI are the sole mechanisms at work, will be used as benchmark later on to help us determine the impact of fading in the NBI suppression process. Results are given in Figure 4, where the use of different wavelet types across different LTE physical channels yields to improved suppression results. Haar wavelets are not recommended for PDSCH because, as shown in Figure 4(a), they introduce performance losses with respect to the 'NBI On' case. Coiflets, in contrast, are clearly the best option, with performance matching that of the 'NBI Off' case. Thanks to the robustness of the Zadoff-Chu sequences conveyed in the PSCH, both Daubechies and Biorthogonal wavelets match the 'NBI Off' case performance in Figure 4(b) also with no single error measured. While this is not the case in Figure 4(c), due to the weaker pseudo-random sequences conveyed in SSCH, Coiflets again outperform all other wavelet types considered.

TABLE II
SIMULATIONS SETTINGS.

SOI Parameters					
N_{S}	Δf	T_{CP}	$1/T_{\text{S}}$	f_{c}	**BW**
512	15kHz	4.69μs	30.72MS/s	465MHz	5MHz
NBI Parameters					
A_i		f_i	f_{dev}	I	**BW**
NBI/SOI=15dB		f_1, f_2	5kHz	$\{0,1\}$	12.5kHz
Wavelet-specific Parameters					
Wavelet Type	**Short Name**	N	L_{sup}	W	
Biorthogonal	Bior9.3	9.3	19.7	20 taps	
Coiflets	Coif-5	5	29	30 taps	
Daubechies	Daub-8	8	15	16 taps	
Haar	Haar	1	1	2 taps	

B. Flat Fading Channel

A second simulation campaign was carried out to determine the performance derived when the received signal is subjected to flat fading, $i.e.$ all of its frequencies are equally affected by the channel. The corresponding results are shown in Figure 5, where we again see that different performances can be derived by employing different wavelets. In Figure 5(a), Daubechies and Coiflets give similar results for PDSCH until SNR about 10 dB, with the latter becoming better than the former from that point on. Figure 5(b) shows that all the types of wavelets but Daubechies perform approximately same. Daubechies offer gains of up to 20 dB over the 'NBI On' case, thus having their selection justified for PSCH. A similar behavior is observed in Figure 5(c), where Coiflets also prove to be an interesting option for SSCH provided that the SNR is high enough.

C. Frequency-selective Fading Channel

3GPP has been developing channel models for LTE. However, to the best of our knowledge, no standardized (nor widely accepted) model reflecting LTE operation in the Band 31 was available at the time of writing. A suitable alternative is the 6-tap channel model established within the IEEE 802.22 standard [15], which meets most requirements mandated by [16] (see Table III). In the sequel, we present a smaller set of results obtained using the 'Profile A' of the 802.22 channel model. One issue brought about by this choice is that the maximum delay spread of 21 μs (see Table IV) cannot be absorbed by the standard CP lengths, $T_{\text{CP}}=N_{\text{S}}/T_{\text{S}}\approx 4.69$ μs for normal CP, and $T_{\text{CP}}=16.67$ μs for extended CP, used in LTE. In this setting, ISI is the dominating effect and less would be seen in terms of NBI suppression regardless the T_{CP} used.

TABLE III
LTE CHANNEL MODEL CONFIGURATION PARAMETERS.

Parameter	**Band 31 [16]**	**IEEE 802.22 [15]**
Transmitter-receiver separation	$\approx$ 30 Km	10-100 Km
Radio frequency	450-470 MHz	30-3000 MHz
Channel bandwdith	5 MHz	5/6/7 MHz
Propagation conditions	LOS, NLOS	LOS, NLOS
Environment type	Rural	Rural, Suburban, Urban
Transmit antenna height	40 m	30-1000 m
Receive antenna height	5-10 m	10 m
Multipath profiles	Not Available	See Table IV
Seasons of operation	All	All

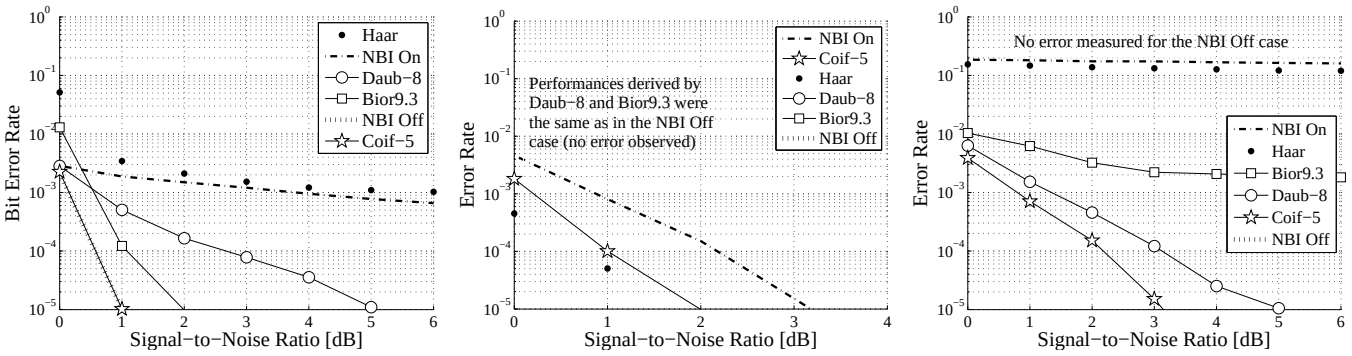

(a) PDSCH @$f_1 = 463.55$MHz (b) PSCH @$f_2 = 464.60$MHz (c) SSCH @$f_2 = 464.60$MHz

Fig. 4. NBI suppression performance obtained over LTE physical channels using different wavelet types in the presence of AWGN only.

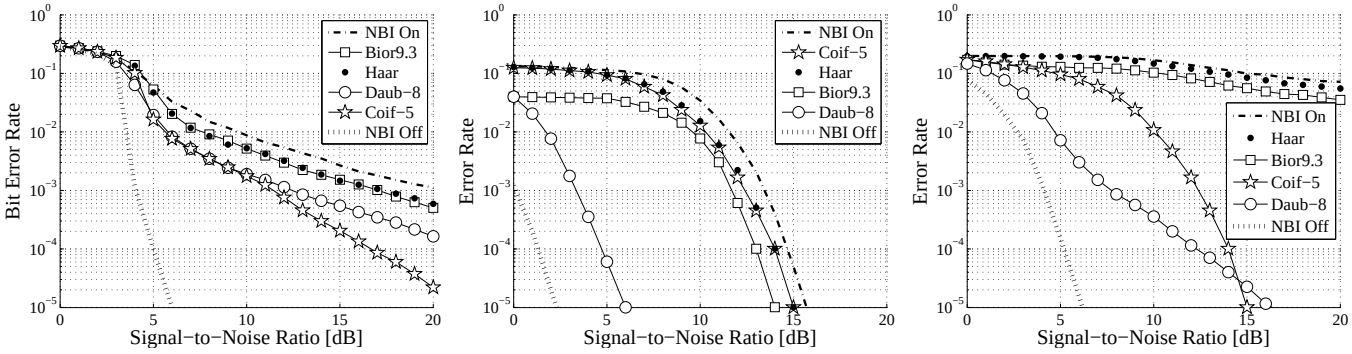

(a) PDSCH @$f_1 = 463.55$MHz (b) PSCH @$f_2 = 464.60$MHz (c) SSCH @$f_2 = 464.60$MHz

Fig. 5. NBI suppression performance obtained over LTE physical channels using different wavelet types in the presence of flat fading.

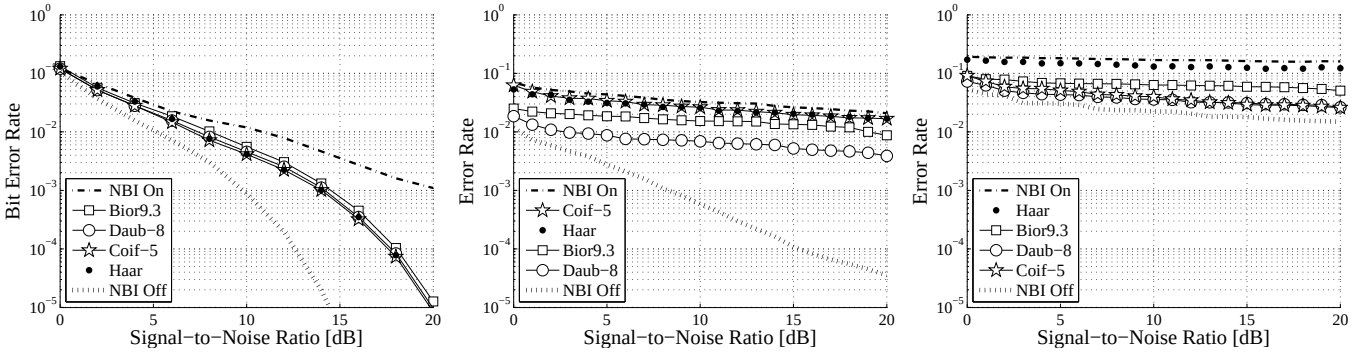

(a) PDSCH @$f_1 = 463.55$MHz (b) PSCH @$f_2 = 464.60$MHz (c) SSCH @$f_2 = 464.60$MHz

Fig. 6. NBI suppression performance obtained over LTE physical channels using different wavelet types in the presence of frequency-selective fading.

To circumvent this limitation, thus allowing the LTE system to work in the ISI-free region, we changed the maximum delay spread to 15 μs, and selected the extended CP. Nevertheless, the benefit of NBI suppression can only be better visualized when ideal channel estimation is used. Under this assumption, Figure 6(a) suggests that any type of wavelet chosen among the candidates considered outperforms the 'NBI On' case in excess of 5 dB. Apparently, and unlike the results just discussed for PDSCH, the assumption of ideal channel estimation seems to play a less critical role for synchronization channels. This is seen for PSCH and SSCH in Figure 6(b) and Figure 6(c), respectively, whose curves are roughly same as those obtained using MMSE channel estimation (not shown in the figures).

TABLE IV
MULTIPATH PROFILE USED IN THE SIMULATIONS OF SECTION III.*C*.

Profile "A"	**Path** 1	**Path** 2	**Path** 3	**Path** 4	**Path** 5	**Path** 6
α_l [dB]	0	-7	-15	-22	-24	-19
σ_l [μs]	0	3	8	11	13	21
f_l [Hz]	0	0.10	2.5	0.13	0.17	0.37

D. Discussion

Table V summarizes the results of all simulation campaigns carried out in this paper. One conclusion drawn from this table is that the optimisation of the NBI suppression process across the LTE physical channels calls for different types of wavelets.

TABLE V
SUMMARY OF SIMULATION RESULTS.

Channel Type	PDSCH	PSCH	SSCH
AWGN	Coif-5	Bior9.3,Daub-8	Coif-5
Flat Fading	Coif-5	Daub-8	Coif-5,Daub-8
Frequency-selective	Coif-5	Daub-8	Coif-5,Daub-8

The use of Coiflets has proven most suitable for cancelling out narrowband signals in the user plan, characterized in terms of PDSCH here. Daubechies have been shown as the best option when it comes to NBI in the control plane, especially in PSCH. As for SSCH, either Coiflets or Daubechies can be applied thanks to their similar suppression performances.

Besides of having determined the matches among physical channels and wavelet types that offer the best NBI suppression results for LTE systems, this paper has illustrated the extent to which the wavelet-based approach depends on the wireless channel considered. In fact, our simulation work suggests that choosing the "right match" yields to ideal performance under AWGN for most physical channels. However, the performance losses (with respect to the ideal 'NBI Off' case) progressively increase as more realistic operation conditions such as shadowing and multipath fading are taken into consideration. This is in good agreement with our expectations, as multiplicative mechanisms create oscillations in the received power level whose contributions have potential to dominate the contribution due to NBI. In this case, the performances observed for scenarios 'NBI Off' and 'NBI On' become so close to each other that the gains derived by using wavelets dramatically decrease.

We believe that these results are, in part, due to the ability to reject frequencies out of the band of interest, and complementarity of the quadrature mirror filters (QMF) pair used in the analysis and synthesis blocks. As shown in Figure 7, Bior9.3 and Haar QMF pairs are respectively the least complementar and weakest in terms of out-of-band attenuation. In contrast,

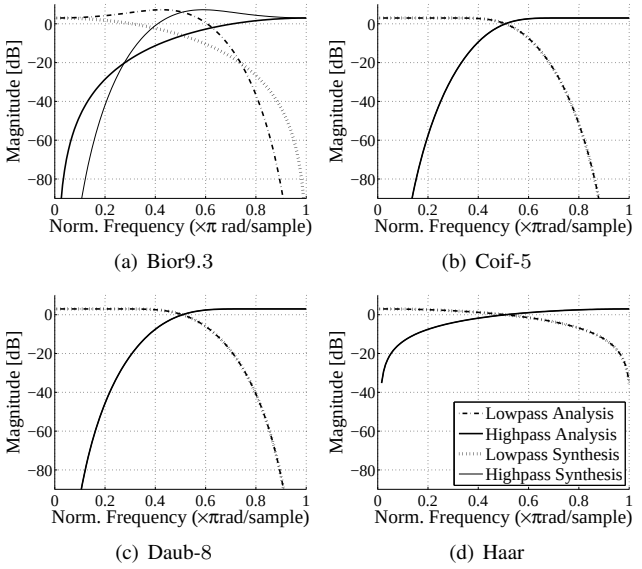

(a) Bior9.3 (b) Coif-5

(c) Daub-8 (d) Haar

Fig. 7. Magnitude responses of the corresponding wavelet filters for a given resolution level. The legend of subplot (d) holds also for subplots (a)–(c).

Coif-5 and Daub-8 are the most complementar and effective QMF pairs. However, recalling that the wavelet choice tightly relates to the SOI, and symmetry (or asymmetry, as in Coiflets and Daubechies) may also play a role in the NBI suppression process, in our future work we will deepen the study by looking into the structures of QPSK signals, Zadoff-Chu sequences and pseudo-random sequences respectively conveyed through PDSCH, PSCH, and SSCH.

IV. CONCLUDING REMARKS

This paper has described a wavelet-based approach aimed at mitigating NBI in LTE physical channels. Our simulations suggest that an optimised NBI suppression process calls for different wavelet types, the choice of which being dependent of the physical channel considered. Daubechies are shown most convenient for synchronization channels (PSCH and SSCH), while Coiflets are found to be the best option when it comes to data shared channels (PDSCH).

ACKNOWLEDGMENT

This material is based upon work supported by FUNTTEL/FINEP under grants 01.12.0481.00 and 01.09.0631.00. The authors are also grateful to Dr. L. C. Pereira for fruitful discussions on the suitability of the 802.22 channel model for simulations in the 3GPP Band 31.

REFERENCES

[1] M. E. Sahin, I. Guvenc and H. Arslan, "An Iterative Interference Cancellation Method for Co-channel Multicarrier and Narrowband Systems", *Physical Communication*, vol. 4, no. 1, pp. 13-25, Mar. 2011.

[2] R. Nilsson, F. Sjoberg and J. P. LeBlanc, "A Rank-Reduced LMMSE Canceller for Narrowband Interference Suppression in OFDM-based Systems", *IEEE Trans. Commun.*, vol.51,no.12,pp.2126-2140, Dec.2003.

[3] A. Gomaa and N. Al-Dhahir, "A Compressive Sensing Approach to NBI Cancellation in Mobile OFDM Systems", *In Proc. of the IEEE Globecom*, pp. 1-5, Dec. 2010.

[4] L. Mei, Q. Zhang, X. Sha and N. Zhang, "WFRFT Precoding for Narrowband Interference Suppression in DFT-based Block Transmission Systems", *IEEE Commun. Lett.*, vol.17, no.10, pp.1916-1919, Oct. 2013.

[5] A. J. Coulson, "Bit Error Rate Performance of OFDM in Narrowband Interference with Excision Filtering", *IEEE Trans. Wireless Commun.*, vol. 5, no. 9, pp. 2484-2492, Sept. 2006.

[6] F. Dovis and L. Musumeci, "Use of Wavelet Transforms for Interference Mitigation", *In Proc. of the ICL-GNSS*, pp. 116-121, June 2011.

[7] W. W. Jones and K. R. Jones, "Narrowband Interference Suppression using Filter-bank Analysis/Synthesis Techniques", *In Proc. of the IEEE Milcom*, vol. 3, pp. 898-902, Oct. 1992.

[8] Y. Zhang, M. G. Amin and A. R. Lindsey, "Anti-jamming GPS Receivers based on Bilinear Signal Distributions", *In Proc. of the IEEE Milcom*, pp. 1070-1074, Oct. 2001.

[9] J. P. Miranda et al., "Narrowband Interference Suppression in Long Term Evolution Systems", *In Proc. of the IEEE PIMRC*, pp. 707-711, Sept. 2014.

[10] 3GPP TS 36.213, "Physical Layer Procedures", Sept. 2012.

[11] 3GPP TS 36.211, "Physical Channels and Modulation", Sept. 2012.

[12] F. Auger, P. Flandrin, P. Goncalves, and O. Lemoine, *Time Frequency Toolbox for Use with Matlab*, CNRS and Rice University, Oct. 2005.

[13] K. K. Shukla and A. K. Tiwari, "Efficient Algorithms for Discrete Wavelet Transform with Applications to Denoising and Fuzzy Inference Systems", Springer 2013.

[14] M. Misiti, Y. Misiti, G. Oppenheim, and J.-M. Poggi, "Wavelet Toolbox – Matlab User's Guide", March 2014.

[15] E. Sofer and G. Chouinard, "WRAN Channel Modeling", IEEE 802.22-05/0055r7, Sept. 2005.

[16] Brazilian National Agency of Communications (ANATEL). Resolution No. 558, "Regulations on channelization and use conditions of radiofrequencies in the 450-470 MHz band [in Portuguese]", Dec. 2010.